PERGAMON

International Journal of Solids and Structures 36 (1999) 2793–2805

INTERNATIONAL JOURNAL OF SOLIDS and STRUCTURES

Finite amplitude spherically symmetric wave propagation in a prestressed hyperelastic shell

J. B. Haddow[a,*], L. Jiang[b]

[a] *Department of Mechanical Engineering, University of Victoria, Victoria, B.C. Canada*
[b] *Martec Ltd. 1888 Brunswick St., Suite 400, Halifax, Nova Scotia, Canada*

Received 20 March 1997; in revised form 11 March 1998

Abstract

Spherically symmetric finite amplitude wave propagation in a prestressed compressible hyperelastic spherical shell is considered. The prestress results from quasi-static application of internal pressure and a numerical solution for this elastostatic problem is obtained first. Dynamic change of the internal pressure results in the propagation of a spherically symmetric wave. A Godunov type finite difference scheme is proposed for the solution of the wave propagation problem and numerical results, which are valid until the first reflection, are presented for a particular isotropic strain energy function and for the special cases of sudden removal and sudden increase of the internal pressure.

1. Introduction

Problems of finite amplitude spherically symmetric wave propagation in hyperelastic solids have been considered by Bland (1969), Janele et al. (1989) and others, and the propagation of infinitesimal waves in a hyperelastic solid with an underlying finite static deformation has been extensively studied. However, the literature contains very little work on the propagation of finite amplitude waves in a hyperelastic solid with an underlying inhomogeneous finite static deformation and the purpose of this paper is to consider such a problem. This problem is finite amplitude spherically symmetric wave propagation in a uniform thick walled spherical compressible hyperelastic shell, which has been subjected initially to finite deformation by a quasi-static application of internal pressure. It is assumed that the wave propagation is due to a sudden change of the initial static internal pressure, including complete and partial removal.

Analytic solutions for the quasi-static inflation of a compressible thick walled hyperelastic shell have been obtained for special strain energy functions by Ogden (1984) and Chung et al. (1986); however, the present authors have been unable to extend these analytic solutions to the wave propagation problem.

* Corresponding author. Fax: 001 250 721 6051; e-mail: jhaddow@me-mailhost.uvic.ca

0020–7683/99/$ - see front matter
PII: S0020–7683(98)00118–8

Numerical results are obtained for the Gaussian strain energy function, which is realistic for a limited range of deformation of a solid rubber, and is given by

$$W = \frac{\mu}{2}\{\lambda_r^2 + \lambda_\theta^2 + \lambda_\phi^2 - 3J^{2/3}\} + \frac{K}{2}\{J-1\}^2, \quad J = \lambda_r\lambda_\theta\lambda_\phi. \tag{1}$$

in terms of the principal stretches λ_r, λ_θ, λ_ϕ referred to spherical polar coordinates (r, θ, ϕ). In (1) μ and K are the shear and bulk moduli, respectively, for infinitesimal deformation from the natural reference configuration. For spherically symmetric deformation $\lambda_\theta = \lambda_\phi$. The term solid rubber is used to denote rubber which has no embedded cavities, unlike foam rubber.

Strain energy function (1) is a compressible generalization of the neo-Hookean model (Ogden, 1982); however, the procedures described are valid for other isotropic compressible strain energy functions. Results are obtained for $K/\mu = 100$ which gives Poisson's ratio $v = 0.495$, for infinitesimal deformation from the natural reference state. Beatty and Stalnaker (1986) have obtained an experimental value of $v = 0.493$ for urethane. Results given by Haddow and Jiang (1996) provide justification for the neglect of thermodynamic effects, that is the use of a purely mechanical theory, for (1) with $K/\mu = 100$.

The static problem is solved numerically, in order to provide the initial conditions for the superimposed wave propagation problem, which is then solved numerically, using a modification of a finite difference scheme due to van Leer (1979).

The analytic solution of Chung et al. (1986) for the static problem is for the Blatz and Ko strain energy function,

$$W = \frac{\mu}{2}(\lambda_r^{-2} + \lambda_\theta^{-2} + \lambda_\phi^{-2} - 2\lambda_r\lambda_\theta\lambda_\phi - 5), \tag{2}$$

which was proposed as a model for foam rubber. Poisson's ration, v, for (2) is 0.25, whereas for a solid rubber v is greater than about 0.45 and in some cases very close to 0.5. The problem of wave propagation in a material such as foam rubber, which has embedded cavities, involves dispersion due to the multiple scattering of the waves from the cavities (Beltzer et al., 1989), and the governing equations, given in this paper, for wave propagation in a solid without cavities or inclusions are not valid. Consequently, results for the wave propagation problem with strain energy function (2) are not given; numerical results for the static problem with (2) were obtained and compared with those from the analytic solution as a check on the numerical procedure.

2. Static solution

A thick walled spherical shell with inner (outer) radius A (B), in the undeformed natural reference configuration is subjected to a quasi-static application of internal pressure and the inner (outer) radius becomes a (b). At this stage it is convenient to introduce the following nondimensionalization scheme for the static problem,

$$\bar{R} = R/A, \quad \bar{A} = 1, \quad \bar{B} = B/A, \quad \bar{r} = r/A, \quad m = K/\mu,$$

and terms with dimension of stress are nondimensionalized by dividing by μ. Henceforth nondimensional quantities are used and the overbars are omitted.

The spherically symmetric static deformation is given by

$$r = r(R), \tag{3}$$

where r and R denote the radial coordinates of a material particle in the current configuration and the undeformed reference configuration, respectively, so that $r(1) = a$ and $r(B) = b$. Principal components of the stretch are given by

$$\lambda_r = r', \quad \lambda_\theta = \lambda_\phi = r/R, \tag{4}$$

where a prime denotes differentiation with respect to R. A Lagrangian representation is used and the principal components of the Biot stress tensor, Ogden (1984), are given by

$$T_R = \frac{\partial W}{\partial \lambda_r}, \quad T_\theta = \frac{\partial W}{\partial \lambda_\theta}, \quad T_\phi = \frac{\partial W}{\partial \lambda_\phi}, \quad T_\phi = T_\theta. \tag{5}$$

Use of the Biot stress results in a simpler derivation of (7) than use of the Cauchy stress. The Lagrangian form of the equilibrium equation is

$$\frac{\mathrm{d}T_R}{\mathrm{d}R} + \frac{2(T_R - T_\theta)}{R} = 0. \tag{6}$$

Substitution of (3)–(5) into (6) gives the nonlinear second order ordinary differential equation for r,

$$\frac{\partial^2 W}{\partial \lambda_r^2} r'' + 2\frac{\partial^2 W}{\partial \lambda_r \partial \lambda_\theta}\left\{\frac{r'}{R} - \frac{r}{R^2}\right\} + \frac{2}{R}\left\{\frac{\partial W}{\partial \lambda_r} - \frac{\partial W}{\partial \lambda_\theta}\right\} = 0, \tag{7}$$

where

$$\begin{aligned}
\frac{\partial W}{\partial \lambda_r} &= m\left\{r' - \left(\frac{r}{R}\right)^2 + \left(\frac{r}{R}\right)^4\right\} - \left(\frac{r}{R}\right)^{4/3} r'^{-1/3}, \\
\frac{\partial W}{\partial \lambda_\theta} &= m\left\{\left(\frac{r}{R}\right)^3 r'^2 - \left(\frac{r}{R}\right) r'\right\} + \frac{r}{R} - \left(\frac{r}{R}\right)^{1/3} r'^{2/3}, \\
\frac{\partial^2 W}{\partial \lambda_r^2} &= 1 + m\left(\frac{r}{R}\right)^4 + \frac{1}{3}\left(\frac{r}{R}\right)^{4/3} r'^{-4/3}, \\
\frac{\partial^2 W}{\partial \lambda_r \partial \lambda_\theta} &= m\left\{2\left(\frac{r}{R}\right)^3 r' - \frac{r}{R}\right\} - \frac{2}{3}\left(\frac{r}{R}\right)^{1/3} r'^{-1/3},
\end{aligned} \tag{8}$$

for strain energy function (1). For the Blatz and Ko strain energy function,

$$\frac{\partial W}{\partial \lambda_r} = \left(\frac{r}{R}\right)^2 - r'^{-3}, \quad \frac{\partial W}{\partial \lambda_\theta} = -\left(\frac{r}{R}\right)^{-3} + \left(\frac{r}{R}\right) r', \quad \frac{\partial^2 W}{\partial \lambda_r^2} = 3r'^{-4}, \quad \frac{\partial^2 W}{\partial \lambda_r \partial \lambda_\theta} = \frac{r}{R},$$

and substitution into (7) gives

$$3R^2r^3r''-2r^3r'R+2R^4r'^4=0, \tag{9}$$

which Chung et al. (1986) reduced to a first order differential equation, by a suitable substitution, and then found an analytic solution. Boundary conditions are

$$T_R(1)=-p_i\lambda_\theta^2(1), \quad T_R(B)=0, \tag{10a,b}$$

or, in terms of the Cauchy stresses,

$$\sigma_r(a)=-p_i, \quad \sigma_r(b)=0,$$

where p_i is the internal pressure. Equation (7) with (8), and eqn (9), were solved numerically, using a Runge–Kutta type method and the results for (9) were found to be in very close agreement with those from the analytic solution.

In order to implement the Runge–Kutta type method, a value of $\lambda_\theta(B)$ and hence $r(B)$ is assumed and the corresponding value of $\lambda_r(B)=r'(B)$ is obtained from boundary condition (10b). A shooting procedure is then used to determine the value of $\lambda_\theta(1)$, required to satisfy the boundary condition (10a). Accurate polynomial approximations for $r=r(R)$ and $T_r=T_R(R)$ were obtained from the numerical solution for use in the numerical scheme for the wave propagation problem.

Results for the static problem were obtained for

$$B=3, \quad T_R(B)=0, \quad \lambda_\theta(B)=1.025, \quad m=100, \tag{11}$$

and these results are shown graphically in Figs 1 and 2. The nondimensional internal pressure corresponding to (11) is

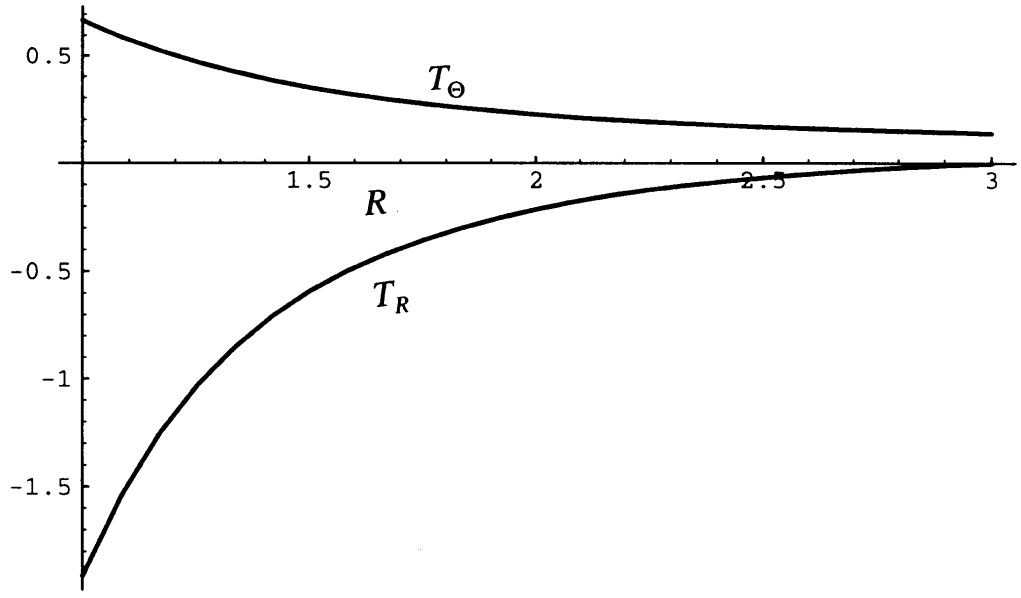

Fig. 1. Biot stress components vs R for the static solution with $B=3$, $T_R(B)=0$ $\lambda_\theta(B)=1.025$, $K/\mu=100$.

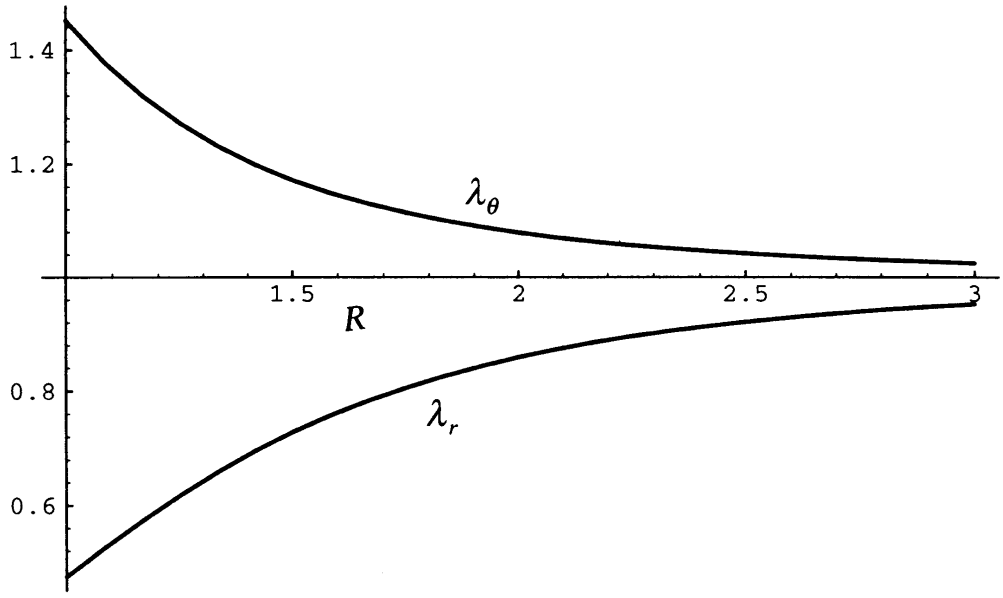

Fig. 2. Stretches λ_r and λ_θ vs R for the static solution with $B = 3$, $T_R(B) = 0$, $\lambda_\theta(B) = 1.025$, $K/\mu = 100$.

$$p_i = -\lambda_\theta(1)^{-2} T_R(1) = 0.912. \tag{12}$$

3. Wave propagation problem

The quantities for the static solution appear in the formulation of the wave propagation problem and in what follows these quantities are denoted by a superposed tilda. In addition to the nondimensionalization scheme for the static problem, time and velocity are nondimensionalized by multiplying by $\sqrt{\mu/\rho_0}/A$ and $\sqrt{\rho_0/\mu}$, respectively, where ρ_0 is the density in the reference configuration.

Initial conditions for the wave propagation problem are

$$r(R,0) = \tilde{r}(R), \quad \mathrm{v}(R,0) = 0, \tag{13}$$

where $\tilde{r}(R)$ is obtained from the numerical solution for the initial static deformation and $v = \partial r(R,t)/\partial t$ is the radial velocity component. The boundary conditions considered are

$$T_R(1,t) = -\lambda_\theta(1,t)^2\{p_i + p_0 H(t)\}, \quad T_R(B,t) = 0, \tag{14}$$

where p_i is given by (12), p_0 is a constant and $H(t)$ is the unit step function. Sudden unloading corresponds to $p_0 = -p_i$. In terms of the Cauchy stress, (14) is given by

$$\sigma_r(a,t) = p_i + p_0 H(t), \quad \sigma_r(b,t) = 0.$$

Governing equations are

$$\frac{\partial T_R}{\partial R}+\frac{2(T_R-T_\theta)}{R}=\frac{\partial v}{\partial t}, \tag{15}$$

$$\frac{\partial \lambda_r}{\partial t}-\frac{\partial v}{\partial R}=0, \tag{16}$$

$$\frac{\partial \lambda_\theta}{\partial t}-\frac{v}{R}=0, \tag{17}$$

which may be put in the form

$$\frac{\partial \mathbf{g}}{\partial t}+\mathbf{A}\frac{\partial \mathbf{g}}{\partial R}+\mathbf{b}=\mathbf{0}, \tag{18}$$

where

$$\mathbf{g}=\begin{bmatrix} v \\ \lambda_r \\ \lambda_\theta \end{bmatrix}, \quad \mathbf{A}=\begin{bmatrix} 0 & -\dfrac{\partial T_R}{\partial \lambda_r} & -\dfrac{\partial T_r}{\partial \lambda_\theta} \\ -1 & 0 & 0 \\ 0 & 0 & 0 \end{bmatrix}, \quad \mathbf{b}=\begin{bmatrix} -\dfrac{2(T_R-T_\theta)}{R} \\ 0 \\ -\dfrac{v}{R} \end{bmatrix} \tag{19}$$

System (18) is strictly hyperbolic and the eigenvalues of $\mathbf{A}$ are $\pm c$ which are the wave velocities and

$$c=\left(\frac{\partial T_R}{\partial \lambda_r}\right)^{1/2}. \tag{20}$$

Jump relations across a shock are

$$V[v]=-[T_R], \quad V[\lambda_r]=-[v], \quad [\lambda_\theta]=0, \tag{21}$$

where V is the shock speed and $[\phi]=\phi_- -\phi_+$, where ϕ_- and ϕ_+ are the values of the enclosed quantity behind and ahead of the shock, respectively. If a shock is initiated at $t=0$ it propagates into a prestressed region and the conditions ahead of the shock are given by the static solution until the first reflection at $R=B$. It follows from (21) that

$$V=\left(\frac{[T_R]}{[\lambda_r]}\right)^{1/2}. \tag{22}$$

In the next section the jump relations (21) are used to develop an approximate Riemann solver based on a finite difference procedure.

For the constitutive relation (1),

$$\frac{\partial^2 T_R}{\partial \lambda_r^2}<0 \quad \text{at } R=1,$$

consequently a shock is initiated at $R=1$ if $p_0>0$ in boundary condition (14) and if $p_0<0$ an

acceleration wave is initiated. The numerical scheme used to obtain solutions for the wave propagation problem has excellent shock capturing properties and the results for the unloading problem, that is $p_0 < 0$, seem to indicate a shock with some smearing. However, for the unloading problem there is a very rapid change of T_R, T_θ, λ_r and v at the wave front which moves, until the first reflection, with the wave speed c, evaluated from the static solution just ahead of the wave front. It follows from (20) that, for strain energy function (1), c is given by

$$c = \sqrt{2}\left\{1 + m\lambda_\theta^4 + \frac{\lambda_\theta^2}{3(\lambda_r\lambda_\theta^2)^{4/3}}\right\}. \tag{23}$$

The term $\sqrt{2}m\lambda_\theta^4$ is dominant in the right hand side of (23) when $m = 100$, consequently, for a fixed value of λ_θ, the variation of c with λ_r is negligible. This is the reason for the very rapid change of T_R, λ_r and v at the wave front. For the loading problem, that is $p_0 > 0$, the jumps and propagation velocity for the shocks indicated by the numerical solutions are in close agreement with (21) and (22).

4. Numerical method for wave propagation problem

The numerical scheme for the wave propagation problem is a Godunov type finite difference scheme. In order to implement this scheme the governing eqn (18) is expressed in the conservation form

$$\frac{\partial \mathbf{g}}{\partial t} + \frac{\partial \mathbf{h}}{\partial R} + \mathbf{b} = \mathbf{0}, \tag{24}$$

where

$$\mathbf{g} = \{v, \lambda_r, \lambda_\theta\}^T, \quad \mathbf{h} = \{-T_R, -v, 0\}^T, \quad \mathbf{b} = \{-2(T_R - T_\theta)/R, 0, -v/R\}^T. \tag{25}$$

and the superposed T denotes transposition. The interval $1 \leqslant R \leqslant B$ is discretized into m equal cells of length ΔR and $1 = R_1 < R_2 < \cdots < R_j < \cdots < R_{m+1} = B$. For a typical time step $t \in [t^n, t^{n+1}]$ and the jth cell $R \in [R_j, R_{j+1}]$, the weak form of the governing equation (24) can be constructed as

$$\int_{t^n}^{t^{n+1}} \int_{R_j}^{R_{j+1}} \left(\frac{\partial \mathbf{g}}{\partial t} + \frac{\partial \mathbf{h}}{\partial R} + \mathbf{b}\right) R^2 \, \mathrm{d}R \, \mathrm{d}t = 0, \tag{26}$$

using the finite volume method. Integrating (26) by parts gives

$$\bar{\mathbf{g}}_{j+1/2}^{n+1} = \bar{\mathbf{g}}_{j+1/2}^{n} - \frac{\Delta t}{\Delta R}(\hat{\mathbf{h}}_{j+1} - \hat{\mathbf{h}}_j) - \Delta t \tilde{\mathbf{b}}_{j+1/2}, \tag{27}$$

where the superposed bar, caret, and tilde denote spatial, time and volume averaged quantities, respectively, and the superscripts and subscripts denote time and space discretizations, respectively. Further approximations for the time averaged values give

$$\bar{\mathbf{g}}_{j+1/2}^{n+1} = \bar{\mathbf{g}}_{j+1/2}^{n} - \frac{\Delta t}{\Delta R}[\mathbf{h}(\hat{\mathbf{g}}_{j+1}) - \mathbf{h}(\hat{\mathbf{g}}_j)] - \Delta t \mathbf{b}\left[\frac{1}{2}(\hat{\mathbf{g}}_{j+1} + \hat{\mathbf{g}}_j)\right], \tag{28}$$

where $\hat{\mathbf{g}}_j\, j \in \{1, 2, \ldots, m+1\}$, is obtained by solving a Riemann problem at each cell interface and by considering the appropriate boundary conditions.

In the present study the numerical scheme was developed by modifying a second-order Godunov-type scheme proposed by van Leer (1979). In the van Leer scheme, state variables at time step t^n are represented by piecewise linear functions of the form

$$\mathbf{g}(R, t^n) = \bar{\mathbf{g}}^n_{j+1/2} + \frac{\overline{\Delta \mathbf{g}^n_{j+1/2}}}{\Delta R}(R - R_{j+1/2}), \quad \text{for } R \in [R_j, R_{j+1}], \tag{29}$$

where $\overline{\Delta \mathbf{g}^n_{j+1/2}}$ denotes the spatial averaged slopes which can be evaluated from the spatial averaged values, $\bar{\mathbf{g}}^n$, in adjacent cells using a monotonic condition. The state variables at the cell boundaries at a half time step can be calculated for the piecewise linear distribution using the Taylor series expansion

$$(\mathbf{g}^{n+1/2}_j)^+ = \bar{\mathbf{g}}^n_{j+1/2} + \frac{\Delta t}{2}\left(\frac{\partial \mathbf{g}}{\partial t}\right)^n_{j+1/2} \frac{-\Delta R}{2}\left(\frac{\partial \mathbf{g}}{\partial R}\right)^n_{j+1/2}, \tag{30a}$$

and

$$(\mathbf{g}^{n+1/2}_{j+1})^- = \bar{\mathbf{g}}^n_{j+1/2} + \frac{\Delta t}{2}\left(\frac{\partial \mathbf{g}}{\partial r}\right)^n_{j+1/2} + \frac{\Delta R}{2}\left(\frac{\partial \mathbf{g}}{\partial R}\right)^n_{j+1/2}, \tag{30b}$$

where the superscript $+(-)$ denotes the state variables at the right (left) side of a cell interface. Substituting system (18) in (30), to eliminate the time derivative term, gives

$$(\mathbf{g}^{n+1/2}_j)^+ = \bar{\mathbf{g}}^n_{j+1/2} - \frac{1}{2}\left[\mathbf{I} + \frac{\Delta t}{\Delta R}\mathbf{A}(\bar{\mathbf{g}}^n_{j+1/2})\right]\overline{\Delta \mathbf{g}^n_{j+1/2}} - \frac{\Delta t}{2}\mathbf{b}(\bar{\mathbf{g}}^n_{j+1/2}), \tag{31a}$$

and

$$(\mathbf{g}^{n+1/2}_{j+1/2})^- = \bar{\mathbf{g}}^n_{j+1/2} + \frac{1}{2}\left[\mathbf{I} - \frac{\Delta t}{\Delta R}\mathbf{A}(\bar{\mathbf{g}}^n_{j+1/2})\right]\overline{\Delta(\mathbf{g}^n_{j+1/2}} - \frac{\Delta t}{2}\mathbf{b}(\bar{\mathbf{g}}^n_{j+1/2}), \tag{31b}$$

where $\mathbf{A}$ and $\mathbf{b}$ are given by (19) and $\mathbf{I}$ is the unit matrix. A Riemann problem is then solved at each interface to resolve the discontinuities between $(\mathbf{g}^{n+1/2}_j)^+$ and $(\mathbf{g}^{n+1/2}_j)^-$, and to obtain the time averaged state, $\hat{\mathbf{g}}_j$ which is required in (28) to calculate the numerical fluxes and source term.

It is well known that the overall accuracy of a Godunov-type finite difference scheme is usually controlled by the order of the spatial discretization and an approximate Riemann solver is sufficient. In the present study an approximate Riemann solver was developed to calculate $\hat{\lambda}_{rj}$ and $\hat{v}_j$ by using the following approximations for the jump relations (21),

$$(c^{n+1/2}_j)^+(\hat{\lambda}_{rj} - (\lambda^{n+1/2}_{rj})^+) + (\hat{v}_j - (\hat{v}^{n+1/2}_j)^+) = 0 \tag{32a}$$

$$(c^{n+1/2}_j)^-(\hat{\lambda}_{rj} - (\lambda^{n+1/2}_{rj})^-) - (\hat{v}_j - (v^{n+1/2}_j)^-) = 0. \tag{32b}$$

In (32), which are identical to the approximate Riemann solver proposed by Roe (1981), V is approximated by c. The time averaged value of λ_θ was approximated by

$$\hat{\lambda}_{\theta j} = \tfrac{1}{2}\{(\lambda_{\theta j}^{n+1/2})^+ + (\lambda_{\theta j}^{n+1/2})^-\}. \tag{33}$$

The following finite difference approximations of the jump relations (21) and the boundary condition (10),

$$(c_1^{n+1/2})^+\{\hat{v}_1 - (v_1^{n+1/2})^+\{T_R(\hat{\lambda}_{r1}, \lambda_\theta) - T_R((\lambda_{r1}^{n+1/2})^+, (\lambda_{\theta 1}^{n+1/2})^+)\} = 0, \tag{34a}$$

$$(c_1^{n+1/2})^+\{\hat{\lambda}_{r1} - (\lambda_{r1}^{n+1/2})^+\} + \{\hat{v}_1 - (v_1^{n+1/2})^+\} = 0, \tag{34b}$$

$$T_R(\hat{\lambda}_{r1}, \lambda_{\theta 1}) - (\hat{\lambda}_{\theta 1})^2(p_i + p_0) = 0, \tag{34c}$$

were used to obtain the time averaged state at the inner surface $R = 1$. Equations (34) are a system of simultaneous nonlinear algebraic equations in $\hat{\lambda}_{r1}$, $\hat{\lambda}_{\theta 1}$, and v_l and were solved using Newton's method. The boundary condition at $R = B$ was considered in a similar manner.

5. Numerical results

Numerical results were obtained for a sudden change of the internal pressure $p_i = 0.912$ for the static solution of (7) with (8) and the data given in (11). Results are presented for two cases, (a) sudden removal of the static internal pressure p_i, that is for $p_i = -p_0$, and (b) sudden increase in internal pressure with $p_i + p_0 = 2.5$.

(a) Plots of T_R, T_θ and v against R for nondimensional times from $t = 0^+$ to $t = 0.15$ are shown in Figs 3–5, respectively. It is clear that, at the wave front, there is a very rapid change of the

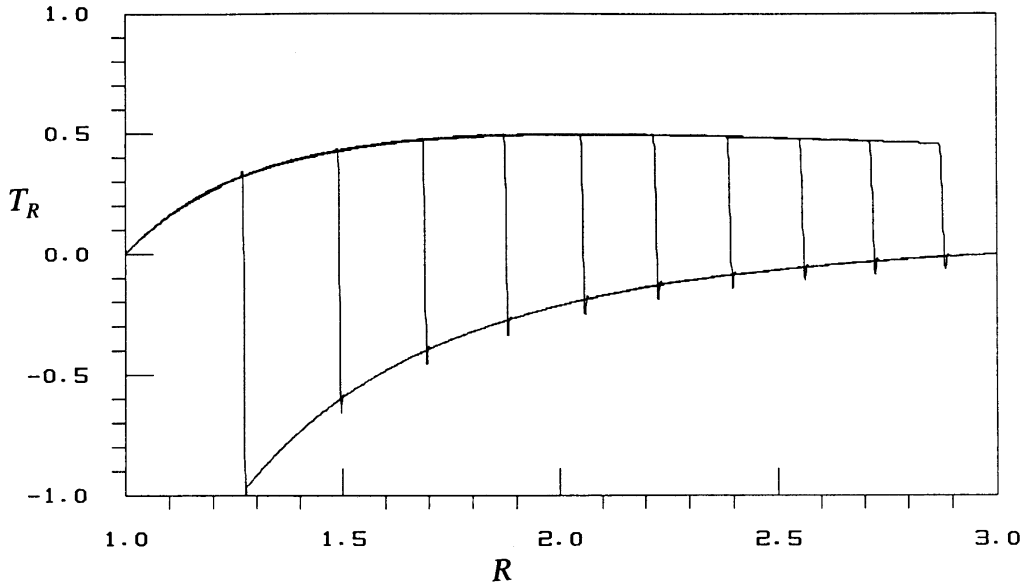

Fig. 3. Biot stress component T_R vs R at intervals 0.015 of nondimensional time, for sudden removal of the internal pressure, $p_i = 0.912$, of the static solution.

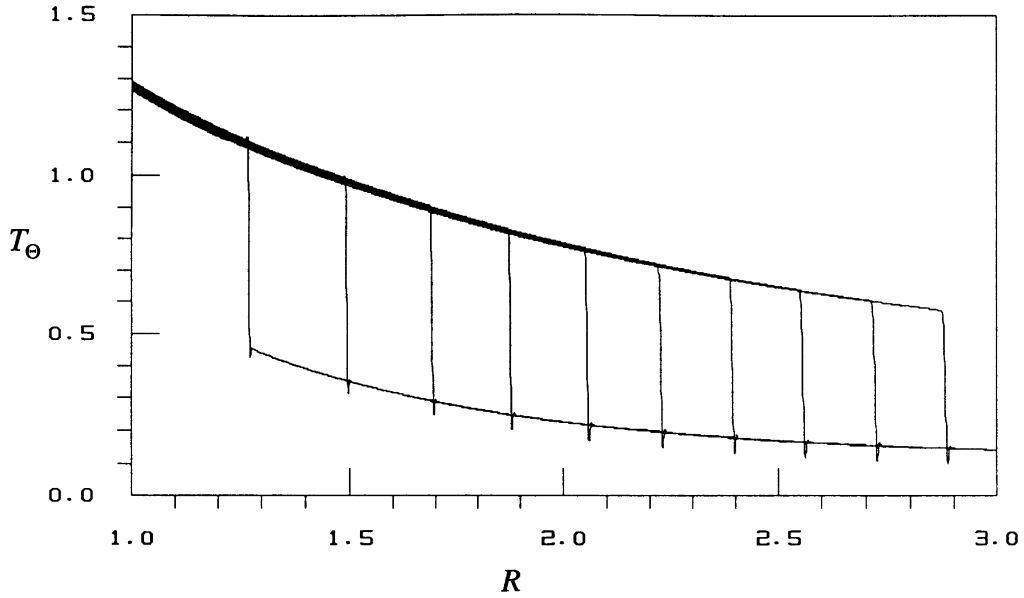

Fig. 4. Biot stress component T_θ vs R at intervals 0.015 of nondimensional time, for sudden removal of the internal pressure, $p_i = 0.912$, of the static solution.

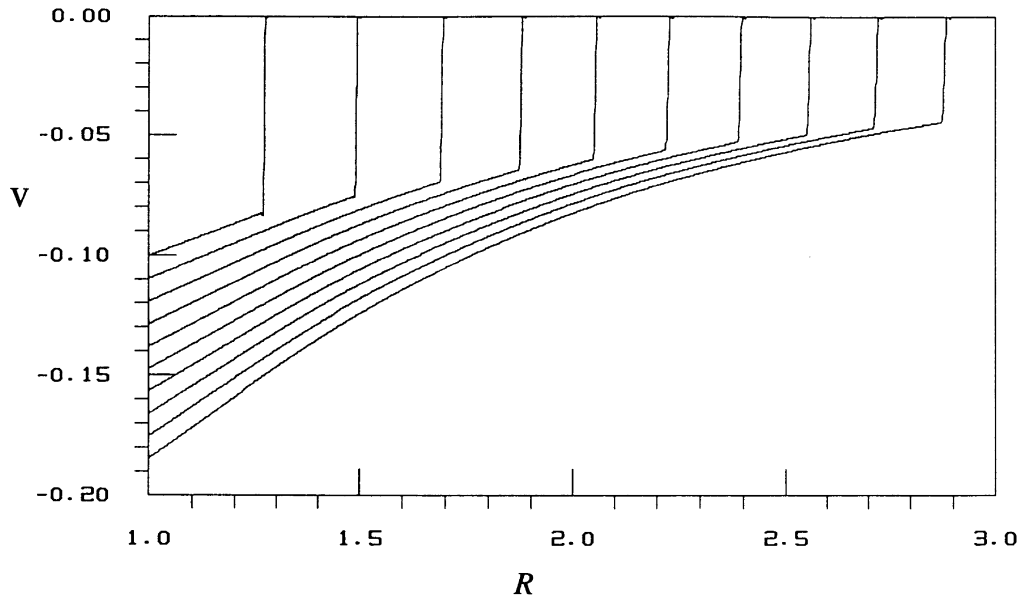

Fig. 5. Radial velocity v vs R at intervals 0.015 of nondimensional time, for sudden removal of the internal pressure, $p_i = 0.912$, of the static solution.

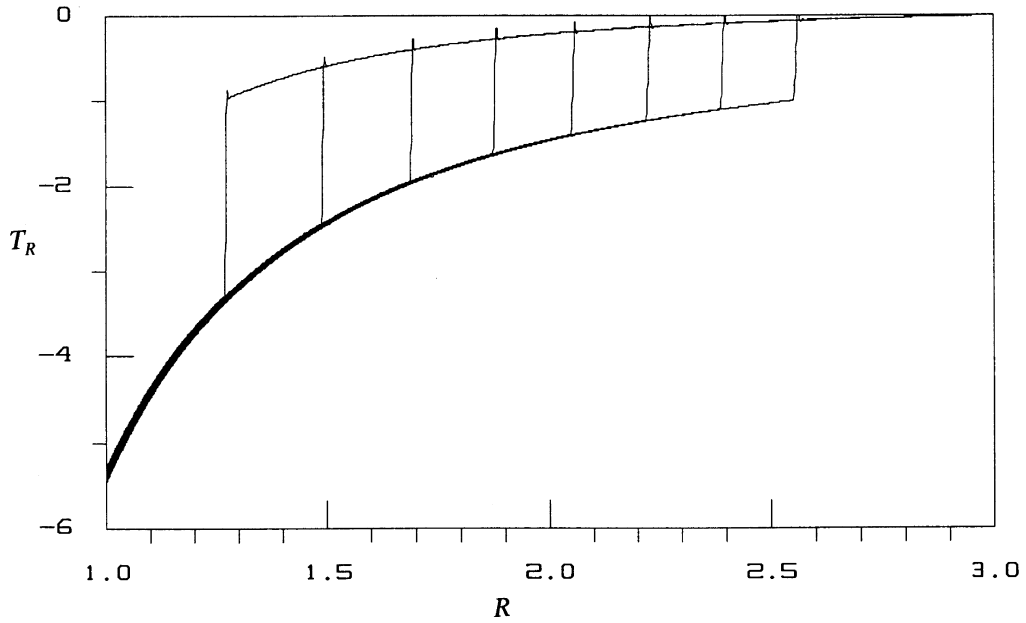

Fig. 6. Biot stress component T_R vs R at intervals 0.015 of nondimensional time for sudden increase of the internal pressure from the static pressure, $p_i = 0.912$, to $p_i + p_0 = 2.5$.

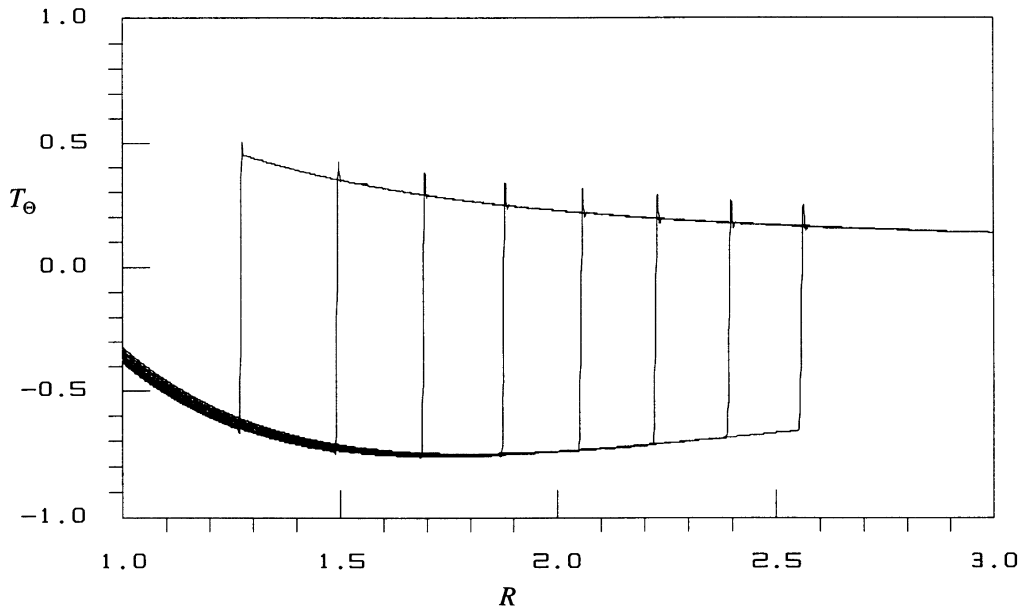

Fig. 7. Biot stress component T_θ vs R at intervals 0.015 of nondimensional time for sudden increase of the internal pressure from the static pressure, $p_i = 0.912$, to $p_i + p_0 = 2.5$.

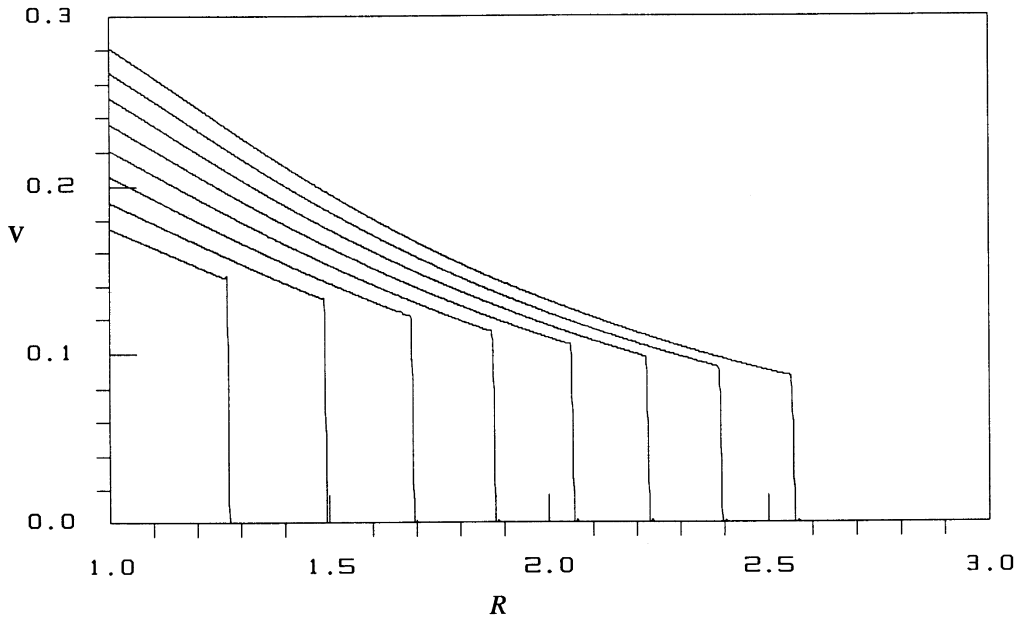

Fig. 8. Radial velocity v vs R at intervals 0.015 of nondimensional time for sudden increase of the internal pressure from the static pressure, $p_i = 0.912$, to $p_i + p_0 = 2.5$.

field variables which has the appearance of a shock. If the wave speed c were a function of λ_θ only, there would be a discontinuity of the field variables at the wave front but the values of c would be the same behind and ahead of the discontinuity. This is similar to what happens in linear elastodynamics when the solid inhomogeneous and a step function change of stress occurs at a boundary. Since the dependence of c on λ_r is very small compared with its dependence on λ_θ, there is a rapid change of the field variables at the wave front; but this is not a shock.

(b) Plots of T_R, T_θ and v against R for nondimensional times from $t = 0^+$ to $t = 0.15$ are shown in Figs 6–8, respectively. The discontinuity indicated at the wave front in Figs 6, 7 and 8 is a genuine shock.

References

Beatty, M.F., Stalnacker, D.O., 1986. The Poisson function of finite elasticity. J. Appl. Mech. 53, 807–813.

Bland, D.R., 1969. Nonlinear Dynamic Elasticity. Blaisdell, New York.

Beltzer, A.I., Wegner, J.L., Haddow, J.B., 1989. Pulse propagation in random media by a causal approach. Bul. Am. Seism. Soc. 79, 113–126.

Chung, D.T., Horgan, C.O., Abeyaratne, R., 1986. The finite deformation of internally pressurized hollow cylinders and spheres for a class of compressible elastic materials. Int. J. Solids Structures 22, 1557–1570.

Janele, P., Haddow, J.B., Mioduchowski, A., 1989. Finite amplitude spherically symmetric wave propagation in a compressible hyperelastic solid. Acta Mech. 79, 25–41.

Haddow, J.B., Jiang, L., 1996. A study of finite amplitude plane wave propagation in a rubberlike-like solid. Wave Motion 24, 211–225.

Ogden, R.W., 1982. Elastic deformations of rubberlike solids. Mechanics of Solids, R. Hill 60th Anniversary Vol. Pergamon Press. pp. 499–537.

Ogden, R.W., 1984. Non-Linear Elastic Deformations. Ellis Horwood.

Roe, P.L., 1981. Approximate Riemann solvers, parameter vectors, and difference schemes. J. Comput. Phys. 43, 357–372.

van Leer, B., 1979. Towards the ultimate conservative difference scheme, V. A second-order sequel to Godunov's method. J. Comp. Phys. 32, 101–136.